

BIFURCATIONS OF SOLITARY WAVES, PERIODIC PEAKONS AND COMPACTONS OF A COUPLED NONLINEAR WAVE EQUATION*

Jinsen Zhuang¹ and Yan Zhou^{1,†}

Abstract For a coupled nonlinear wave equation system, its travelling wave system just is a singular traveling wave system of the first class depending on nine parameters. By using the bifurcation theory and method of dynamical systems and the theory of singular traveling wave systems, in this paper, we show that there exist parameter groups such that this singular system has kink and anti-kink wave solutions, periodic solutions, periodic peakons and compactons as well as different solitary wave solutions.

Keywords Singular travelling wave system, periodic peakon, compacton, solitary wave, bifurcation, coupled nonlinear wave equation.

MSC(2010) 34C37, 34C23, 74J30, 58Z05.

1. Introduction

Nonlinear differential equations can be used to describe many complex natural phenomena. Lots of works have been done to seek possible exact solutions for these nonlinear evolve equations in various fields of mathematical physics (see, e.g. [1, 3, 4, 7–11, 19]). Several effective methods in searching for exact solutions of different nonlinear equations have been used, such as Backlund and Darboux transformation approach [4, 7, 9], variable separation approach [10, 19], etc..

Additionally, the coupled equations also been used to solve different mathematical physical problems. Recently, the study of coupled KdV equations has attracts a lot of attention. The existence of different exact solutions for these coupled KdV equations have been proved (see [5, 6, 12, 13, 20, 21]). Unfortunately, very little research has been done on the generalized system of coupled KdV equations in the form:

$$u_t + \alpha v^2 v_x + \beta u^2 u_x + \lambda u u_x + \gamma u_{xxx} = 0, \quad v_t + \delta (uv)_x + \epsilon v v_x = 0, \quad (1.1)$$

where $\alpha, \beta, \gamma, \delta, \lambda$ and ϵ are any arbitrary constants. According to [5], under certain conditions, if $v = 0$, Eqs.(1.1) turns to KdV and mKdV. Actually, Eqs.(1.1) is generally used in solid-state physics, plasma physics, hydro physics, quanta field theory and so on.

[†]The corresponding author. Email address: zy4233@hqu.edu.cn(Y. Zhou)

¹School of Mathematical Sciences, Huaqiao University, Quanzhou, Fujian 362021, China

*This research was partially supported by the National Natural Science Foundation of China (11571318) and Natural Science Foundation of Fujian Province (2021J01303).

Guha-Roy [5, 6] supposed $|\xi| = |x - ct| \rightarrow +\infty$ with $u(\xi), u'(\xi), u''(\xi) \rightarrow 0$. They used transformation $u(\xi) = \frac{1}{\phi(\xi)}$ and Weierstrass ellipse function, to obtain some exact solitary wave solutions in special conditions. In Shang [20], Xu [21] and Lu [12], by using the ansatz method, they obtained some exact traveling wave solutions of (1.1). Liu [13] used different undermined coefficient methods to obtain some bell-shaped and kink-shaped solitary wave solutions. However, the singular nonlinear traveling wave system corresponding to Eqs.(1.1) can not be found, and more general conclusions about the qualitative properties of the exact traveling solutions have not been given.

Different from the above references, in this paper, by using dynamical system method, we find the singular nonlinear traveling wave system corresponding to (1.1), under certain parameter conditions. It is important to note that singular traveling system may be exist peakon, pseudo-peakon, periodic peakon, compacton solution families as well as many new traveling wave solutions(see [14, 15, 18]). Therefore, depending on the parameters group of Eqs.(1.1), by using the bifurcation theory of the singular nonlinear traveling wave system, we find many new exact traveling wave solutions of Eqs.(1.1), including some solitary wave solutions, periodic wave solutions, kink and anti-kink wave solutions, four different periodic peakons and several compactons, which can not be found in the regular traveling wave system.

Considering traveling wave solutions of Eqs.(1.1), we suppose that $u(x, t) = u(x - ct) = u(\xi), v(x, t) = v(x - ct) = \phi(\xi)$. Substituting them into (1.1) and integrating obtained results once, we have

$$-cu + \frac{1}{3}\alpha\phi^3 + \frac{1}{3}\beta u^3 + \frac{1}{2}\lambda u^2 + \gamma u'' - g_1 = 0, \quad u = \frac{g + c\phi - \frac{\epsilon}{2}\phi^2}{\delta\phi}, \quad (1.2)$$

where g_1 and g are two integral constants. Substituting u given by the second equation of (1.2) into the first equation of (1.2), the general equation is as follows:

$$\phi \left(\frac{1}{2}\epsilon\phi^2 + g \right) \phi'' = 2g(\phi')^2 + a_0 + a_1\phi + a_2\phi^2 + a_3\phi^3 + a_4\phi^4 + a_5\phi^5 + a_6\phi^6, \quad (1.3)$$

where

$$\begin{aligned} a_0 &= \frac{g^3\beta}{3\gamma\delta^2}, \quad a_1 = \frac{g^2}{2\gamma\delta^2}(2\beta c + \lambda\delta), \quad a_2 = \frac{g}{2\gamma\delta^2}(2c^2\beta + 2c\lambda\delta - 2c\delta^2 - g\beta\epsilon), \\ a_3 &= \frac{1}{6\gamma\delta^2}(3c^2\lambda\delta + 2c^3\beta - 6c^2\delta^2 - 6cg\beta\epsilon - 3g\delta\lambda\epsilon - 6g_1\delta^3), \\ a_4 &= -\frac{\epsilon}{4\gamma\delta^2}(2c\delta\lambda + 2c^2\beta - g\beta\epsilon - 2c\delta^2), \\ a_5 &= \frac{\epsilon^2}{8\gamma\delta^2}(2c\beta + \delta\lambda), \quad a_6 = \frac{1}{24\gamma\delta^2}(8\alpha\delta^3 - \beta\epsilon^3). \end{aligned}$$

For $g \neq 0$, equation (1.3) is equivalent to the following planar dynamical system:

$$\frac{d\phi}{d\xi} = y, \quad \frac{dy}{d\xi} = \frac{2gy^2 + a_0 + a_1\phi + a_2\phi^2 + a_3\phi^3 + a_4\phi^4 + a_5\phi^5 + a_6\phi^6}{\phi(\frac{1}{2}\epsilon\phi^2 + g)}, \quad (1.4)$$

which has the first integral

$$H(\phi, y) = \frac{(\epsilon\phi^2 + 2g)^2 y^2}{\phi^4} - \left(a_6\epsilon\phi^4 + \frac{4}{3}a_5\epsilon\phi^3 + 2(a_4\epsilon + 2a_6g)\phi^2 + 4(a_3\epsilon + 2a_5g)\phi - \frac{4(a_1\epsilon + 2a_3g)}{\phi} - \frac{2(a_0\epsilon + 2a_2g)}{\phi^2} - \frac{8a_1g}{3\phi^3} - \frac{2a_0g}{\phi^4} \right) = h. \tag{1.5}$$

Obviously, when $g \neq 0$, system (1.4) is a singular nonlinear traveling wave system of the first class defined in [14] and [15] with three singular straight lines $\phi = 0$ and $\phi = \pm\sqrt{\frac{-2g}{\epsilon}}$, when $g\epsilon < 0$.

If we take $g = 0$, then $a_0 = a_1 = a_2 = 0$. System (1.4) becomes a regular planar Hamiltonian system as follows:

$$\frac{d\phi}{d\xi} = y, \quad \frac{dy}{d\xi} = \frac{2}{\epsilon}(a_3 + a_4\phi + a_5\phi^2 + a_6\phi^3). \tag{1.6}$$

This system has Hamiltonian

$$H_0(\phi, y) = \frac{1}{2}y^2 - \frac{2}{\epsilon} \left(a_3\phi + \frac{1}{2}a_4\phi^2 + \frac{1}{3}a_5\phi^3 + \frac{1}{4}a_6\phi^4 \right). \tag{1.7}$$

We notice that the authors assume that $v = Au + B$ and $k = 0$ in Lu [12] and Liu [13], respectively. These cases just corresponds to our case $g = 0$, i.e., the regular case. Therefore, system (1.6) can not have periodic peakon solutions and compacton solutions.

System (1.4) is a nine-parameter singular traveling system and has high order nonlinearity. It has very abundant dynamical behavior. In this paper, we first consider the case of $g_1 = 0, a_6 = a_5 = a_3 = a_1 = 0$. By taking $\alpha = \frac{\beta\epsilon^3}{8\delta^3}, \beta = -\frac{\delta\lambda}{2c}, \delta = \frac{1}{3}\lambda$, we have

$$a_0 = -\frac{g^3}{2c\gamma}, a_2 = \frac{g}{2\gamma} \left(c + \frac{3g\epsilon}{2c} \right), a_4 = -\frac{\epsilon}{4\gamma} \left(c + \frac{3g\epsilon}{2c} \right).$$

System (1.4) becomes the following four-parameter (c, g, γ, ϵ) singular traveling system:

$$\frac{d\phi}{d\xi} = y, \quad \frac{dy}{d\xi} = \frac{8c\gamma\gamma y^2 - 2g^3 + 2g\hat{\alpha}\phi^2 - \epsilon\hat{\alpha}\phi^4}{2c\gamma\phi(\epsilon\phi^2 + 2g)} \tag{1.8}$$

where $\hat{\alpha} = c^2 + \frac{3}{2}g\epsilon$. System (1.8) has the first integral:

$$H(\phi, y) = \frac{(\epsilon\phi^2 + 2g)^2 y^2}{\phi^4} - \frac{1}{c\gamma} \left(\frac{g^4}{\phi^4} - \frac{2g^2(g\epsilon + c^2)}{\phi^2} - \frac{2c^2\epsilon^2 + 3g\epsilon^3}{4}\phi^2 \right) = h. \tag{1.9}$$

The different phase portrait orbits of system (1.8) in the phase plane (ϕ, y) correspond to different traveling wave solutions $\phi(\xi)$. We will study these traveling wave solutions $\phi(\xi)$ and their dynamic behaviors by analysing bifurcations of phase portraits of (1.8) depending on the parameters c, g, γ, ϵ .

2. Bifurcations of phase portraits of system (1.8)

In this section, we consider bifurcations of phase portraits of system (1.8) depending on the parameter group (c, g, γ, ϵ) . The associated regular system of system (1.8) is as follows:

$$\frac{d\phi}{d\zeta} = 2c\gamma\phi(\epsilon\phi^2 + 2g)y, \quad \frac{dy}{d\zeta} = 8cg\gamma y^2 - 2g^3 + 2g\hat{\alpha}\phi^2 - \epsilon\hat{\alpha}\phi^4, \quad (2.1)$$

where $d\xi = 2c\gamma\phi(\epsilon\phi^2 + 2g)d\zeta$, for $\phi(\epsilon\phi^2 + 2g) \neq 0$.

Because system (2.1) has the same first integrals as that of system (1.8) except the vector fields direction (see [18]), we will obtain the phase portraits of (1.8) by investigating the equilibrium points and bifurcations of phase portraits of system (2.1).

We suppose that $cg\gamma\epsilon \neq 0$. Clearly, if $c\gamma > 0$, then there exist two equilibrium points $N_{1,2}(0, \pm y_0)$ of system (2.1) in the y -axis, where $y_0 = \frac{|g|}{2\sqrt{c\gamma}}$. If $g\epsilon < 0$ and $Y_s = \frac{g(c^2 + \frac{7}{4}g\epsilon)}{c\gamma\epsilon} > 0$, then there exist two equilibrium points $S_{1,2}(-\phi_s, \pm\sqrt{Y_s})$ and $S_{3,4}(\phi_s, \pm\sqrt{Y_s})$ in the two straight lines $\phi = \pm\phi_s = \pm\sqrt{-\frac{2g}{\epsilon}}$, respectively.

Write that $f(\phi) = \epsilon\hat{\alpha}\phi^4 - 2g\hat{\alpha}\phi^2 + 2g^3$, $\Delta = g^2\hat{\alpha}(c^2 - \frac{1}{2}g\epsilon)$. Hence, when $\phi^2 = \phi_{1,2}^2 = \frac{1}{\epsilon} \left(g \pm \frac{\sqrt{\Delta}}{\alpha} \right)$, we have $f(\phi_{1,2}) = 0$, where $\phi_1 < \phi_2$.

Let $M(\phi_j, y_j)$ be the coefficient matrix of the linearized system of system (2.1) at an equilibrium point $E(\phi_j, y_j)$ and $J(\phi_j, y_j) = \det M(\phi_j, y_j)$. We have

$$\begin{aligned} J(\phi_j, 0) &= 2c\gamma\phi_j(\epsilon\phi_j^2 + 2g)f'(\phi_j), \\ J(0, y_0) &= 16c\gamma g^4 > 0, \quad J(\phi_s, \sqrt{Y_s}) = -128c^2\gamma^2g^2Y_s^2 < 0, \\ (\text{trace}M(\phi_j, 0))^2 - 4J(\phi_j, 0) &= -4J(\phi_j, 0), \\ (\text{trace}M(0, y_0))^2 - 4J(0, y_0) &= 36c\gamma g^4 > 0. \end{aligned}$$

By the theory of planar dynamical systems (see [18]), We notice that the equilibrium point $E_j(\phi_j, 0)$ is either a saddle point or a center point. The equilibrium points $N_{1,2}(0, y_0)$ are nodes because $c\gamma > 0$. The equilibrium points $S_{1,2}$ and $S_{3,4}$ are saddle points. In the meantime, we write that $h_j = H(\phi_j, 0)$, $h_s = H(\pm\phi_s, \pm\sqrt{Y_s}) = -\frac{2g\epsilon}{c\gamma}(c^2 + \frac{11}{8}g\epsilon)$ and $h_0 = H(0, \pm y_0) = \infty$, where $H(\phi, y)$ is defined by (1.9).

(1). Assume that $g\epsilon > 0$, thus, system (1.8) only has one singular straight line $\phi = 0$, and $\hat{\alpha} > 0$, then the condition $c^2 - \frac{1}{2}g\epsilon > 0$ implies that $\Delta > 0$.

(i) When $c\gamma > 0$, we have phase portraits Fig.1. (there are two symmetric node points $N_{1,2}(0, \pm y_0)$ of system (2.1) in y -axis)

(ii) When $c\gamma < 0$, we have phase portraits Fig.2. (there is no equilibrium point of system (2.1) in y -axis)

(2). Assume that $g\epsilon < 0$, system (1.8) has three singular straight lines $\phi = 0$ and $\phi = \pm\phi_s = \pm\sqrt{-\frac{2g}{\epsilon}}$, and $c^2 - \frac{1}{2}g\epsilon > 0$, then the condition $\hat{\alpha} > 0$ implies that $\Delta > 0$.

(i) When $c\gamma > 0$, we have phase portraits Fig.3. (there are two symmetric node points $N_{1,2}(0, \pm y_0)$ of system (2.1) in y -axis)

(ii) When $c\gamma < 0$, we have phase portraits Fig.4. (there is no equilibrium point of system (2.1) in y -axis)

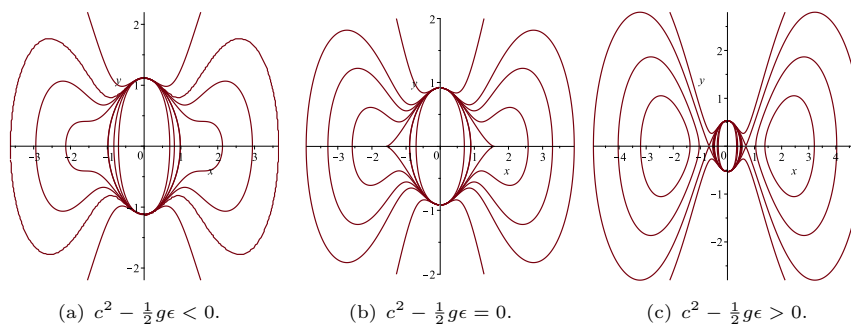


Figure 1. The phase portrait of system (1.8) for $g\epsilon > 0, c\gamma > 0$.

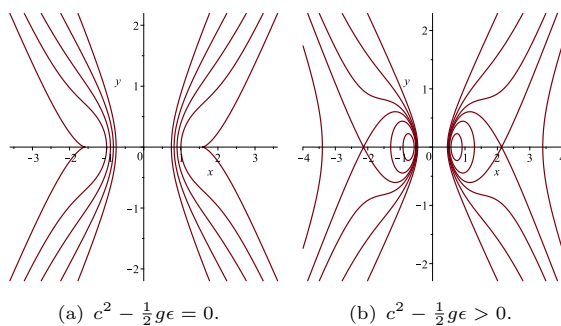


Figure 2. The phase portrait of system (1.8) for $g\epsilon > 0, c\gamma < 0$.

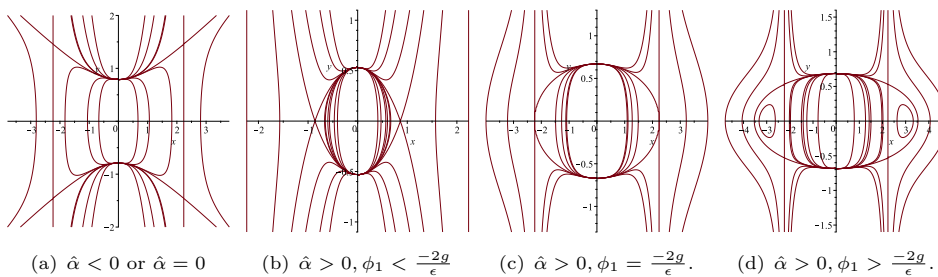


Figure 3. The phase portrait of system (1.8) for $g\epsilon < 0, c\gamma > 0$.

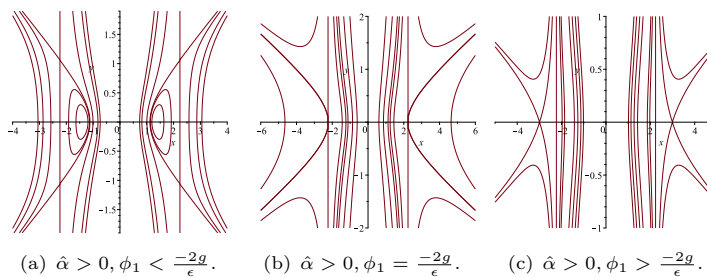


Figure 4. The phase portrait of system (1.8) for $g\epsilon < 0, c\gamma < 0$.

Considering the physical significance, we only discuss the solutions of system (1.8) corresponding to the bounded orbits shown in Fig.1-Fig.4. Then, we can obtain the following conclusions:

(i) When $g\epsilon > 0$ and $c\gamma > 0$, System (1.8) exist uncountable infinite many periodic wave solutions (see Fig.1 (a), (b), (c)), two pairs of different kink and anti-kink wave solutions (see Fig.1 (b), (c)), and two symmetrical solitary wave solution (see Fig.1 (c)).

(ii) When $g\epsilon > 0$ and $c\gamma < 0$, System (1.8) exist two family of periodic wave solutions and two symmetrical solitary wave solution (see Fig.2 (b)).

(iii) When $g\epsilon < 0$ and $c\gamma > 0$, System (1.8) exist uncountable infinite many periodic wave solutions including large amplitude periodic wave solutions and small amplitude periodic wave solutions (see Fig.3 (a), (b), (c), (d)), a pair of kink and anti-kink wave solutions (see Fig.3 (b)), different types of periodic peakon solutions (see Fig.3 (a),(d)), and many compacton solutions.

(iv) When $g\epsilon < 0$ and $c\gamma < 0$, System (1.8) exist two families of symmetrical periodic wave solutions, one lower peakon solution and one upper peakon solution (see Fig.4 (a)), and some compacton solutions.

Remark 2.1. Under some appropriate parameter conditions, system (2.1) will exist saddle points or nodes. If there are nodes in singular straight line, system might exist periodic orbits which give rise to periodic wave solutions of system (1.8). If there are saddle points in singular straight line, system might exist triangle orbits or arched orbits which give rise to peakons and periodic peakons, respectively. Furthermore, when system (1.8) has three singular straight lines, saddle points and nodes of system (2.1) maybe appear in different singular lines at the same time (see Fig.3 (a),(d)), system (1.8) might exist rectangular periodic closed orbits which give rise to the sawtooth periodic peakons.

3. Exact parametric representations of solutions of system (1.8)

In this section, we obtain the exact parametric representations of the solutions mentioned in the above conclusion, by studying the different bounded orbits shown in Fig.1-Fig.4. The following discussion will give the main results.

The first integral $H(\phi, y) = h$ can be written as

$$y^2 = \frac{\beta\phi^6 + h\phi^4 - \frac{2g^2(c^2+g\epsilon)}{c\gamma}\phi^2 + \frac{1}{c\gamma}}{(\phi^2 + \frac{2g}{\epsilon})^2}, \quad \beta = \frac{-(2c^2 + 3g\epsilon)}{4c\gamma} = \frac{-\hat{\alpha}}{2c\gamma}. \quad (3.1)$$

Theorem 3.1. When $g\epsilon > 0$ and $c\gamma > 0$, corresponding to different bounded orbits in Fig.1 (a), (b), (c), system (1.8) has different exact explicit solutions (3.4)-(3.10).

Proof. (i) The case of $c^2 - \frac{1}{2}g\epsilon < 0$.

System (1.8) has the phase portrait Fig.1 (a) and $\beta < 0$. The level curves defined by $H(\phi, y) = h, h \in (-\infty, \infty)$ is a family of global closed orbits which pass ϕ -axis at points $(\pm r_1, 0)$, we obtain from the first equation of system (1.8) that

$$\sqrt{|\beta|}\xi = \int_0^\phi \frac{(\phi^2 + \frac{2g}{\epsilon})d\phi}{\sqrt{(r_1^2 - \phi^2)(\phi^2 - \rho^2)(\phi^2 - \bar{\rho}^2)}}, \quad (3.2)$$

where ρ is a complex number. Let $u = \phi^2$, (3.2) become

$$2\sqrt{|\beta|}\xi = \int_0^u \frac{(u + \frac{2g}{\epsilon})du}{\sqrt{(r_1^2 - u)u(u - \rho^2)(u - \bar{\rho}^2)}}. \tag{3.3}$$

By calculating the integration (3.3), we obtain the following parametric representation of the periodic solutions:

$$\begin{aligned} \phi(\chi) &= \pm \left(\frac{r_1^2 B(1 - \text{cn}(\chi, k))}{(A - B)\text{cn}(\chi, k) + A + B} \right)^{\frac{1}{2}}, \\ \xi(\chi) &= \frac{1}{2\sqrt{|\beta|AB}} \left[\left(\frac{2g}{\epsilon} - \frac{r_1^2 B}{A - B} \right) \chi + \frac{r_1^2}{2\alpha_1} \pi(\arccos(\text{cn}(\chi, k)), \frac{\alpha_1^2}{\alpha_1^2 - 1}, k) - \frac{r_1^2}{2} f_1 \right], \end{aligned} \tag{3.4}$$

where $a_1^2 = -\frac{1}{4}(\rho^2 - \bar{\rho}^2)^2, b_1 = \frac{1}{2}(\rho^2 + \bar{\rho}^2), A^2 = (r_1^2 - b_1)^2 + a_1^2, B^2 = b_1^2 + a_1^2, k^2 = \frac{r_1^4 - (A - B)^2}{4AB}, \alpha_1 = \frac{A - B}{A + B}$. $\text{cn}(\cdot, k), \text{sn}(\cdot, k), \text{dn}(\cdot, k)$ are Jacobin elliptic functions, $\Pi(\cdot, \cdot, k)$ is the elliptic integral of the third kind, the function $f_1(\chi)$ can be seen in [2].

(ii) The case of $c^2 - \frac{1}{2}g\epsilon = 0$.

System (1.8) has the phase portrait Fig.1 (b) and $\beta < 0$. The level curves defined by $H(\phi, y) = h_1$ are two heteroclinic orbits enclosing the origin (0, 0) and connecting two equilibrium points $(\pm\phi_1, 0)$. We have $\sqrt{|\beta|}\xi = \int_0^\phi \frac{(\phi^2 + \frac{2g}{\epsilon})d\phi}{\sqrt{(\phi_1^2 - \phi^2)^3}} = \left[-\int_0^\phi \frac{d\phi}{\sqrt{\phi_1^2 - \phi^2}} + (\phi_1^2 + \frac{2g}{\epsilon}) \int_0^\phi \frac{d\phi}{(\phi_1^2 - \phi^2)\sqrt{\phi_1^2 - \phi^2}} \right]$, and obtain the parametric representations of the kink and anti-kink wave solutions:

$$\begin{aligned} \phi(\chi) &= \phi_1 \sin x, \chi \in \left(-\frac{\pi}{2}, \frac{\pi}{2}\right), \\ \xi(\chi) &= \frac{1}{\sqrt{|\beta|}} \left[-\chi + \left(1 + \frac{2g}{\epsilon\phi_1^2}\right) \tan \chi \right]. \end{aligned} \tag{3.5}$$

(iii) The case of $c^2 - \frac{1}{2}g\epsilon > 0$.

System (1.8) has the phase portrait Fig.1 (c) in which the phase orbits are very rich, and $\beta < 0$. The following Fig.5 (a)-(e) show the changes of the level curves:

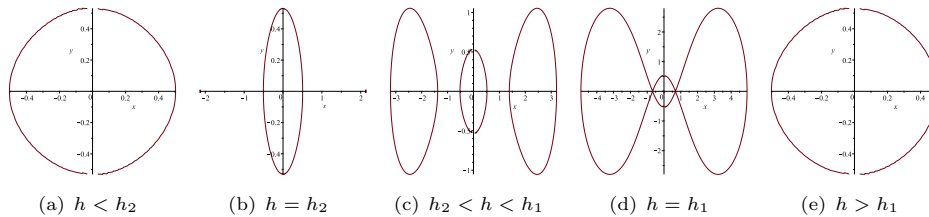


Figure 5. The changes of the level curves for $g\epsilon > 0, c\gamma > 0, c^2 - \frac{1}{2}g\epsilon > 0$.

The level curves defined by $H(\phi, y) = h, h_1 < h < h_2$ (see Fig.5 (a) and (e)) are the same as those of the case (i) in theorem 1.

The level curves defined by $H(\phi, y) = h_2$ are two equilibrium points $(\pm\phi_2, 0)$, and one periodic orbit enclosing $(0, 0)$ and passing ϕ -axis at points $(\pm r_1, 0)$ where $r_1 < \phi_2$ (see Fig.5 (b)). For the periodic orbit, $\sqrt{|\beta|}\xi = \int_0^\phi \frac{(\phi^2 + \frac{2g}{\epsilon})d\phi}{\sqrt{(r_1^2 - \phi^2)(\phi_2^2 - \phi^2)^2}} = \left[-\int_0^\phi \frac{d\phi}{\sqrt{r_1^2 - \phi^2}} + (\phi_2^2 + \frac{2g}{\epsilon}) \int_0^\phi \frac{d\phi}{(\phi_2^2 - \phi^2)\sqrt{r_1^2 - \phi^2}} \right]$. We have the parametric representation of the periodic solution as follows(see Fig.6 (a)):

$$\begin{aligned} \phi(\chi) &= \pm \left(\phi_2^2 - \frac{2\phi_2^2(r_1^2 - \phi_2^2)}{r_1^2 \cos(\omega_1\chi) - 2\phi_2^2 + r_1^2} \right)^{\frac{1}{2}}, \\ \xi(\chi) &= \frac{-1}{\sqrt{|\beta|}} \left[\arcsin \frac{\phi}{r_1} + \frac{1}{2}(\phi_2^2 + \frac{2g}{\epsilon})\chi \right], \end{aligned} \tag{3.6}$$

where $\omega_1 = \phi_2\sqrt{\phi_2^2 - r_1^2}$.

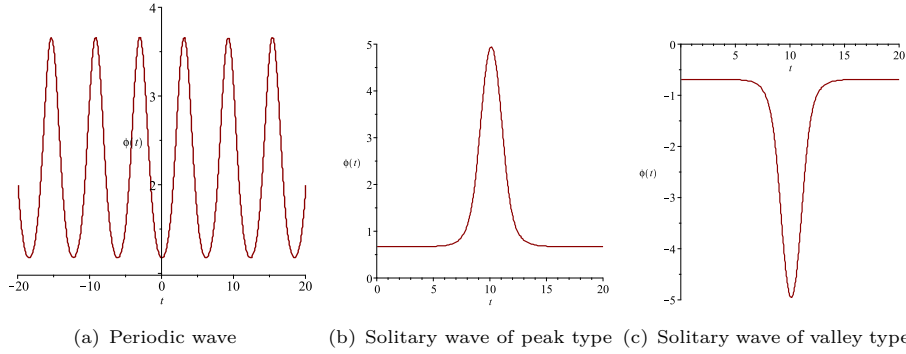


Figure 6. The periodic wave and solitary wave of system (1.8).

The level curves defined by $H(\phi, y) = h, h_2 < h < h_1$ are three families of periodic orbits enclosing $(0, 0)$ and two equilibrium points $(\pm\phi_2, 0)$ respectively (see Fig.5 (c)). For the periodic orbits that encloses the origin point and pass ϕ -axis at points $(\pm r_3, 0)$, $\sqrt{|\beta|}\xi = \int_0^\phi \frac{(\phi^2 + \frac{2g}{\epsilon})d\phi}{\sqrt{(r_1^2 - \phi^2)(r_2^2 - \phi^2)(r_3^2 - \phi^2)}}$. Let $u = \phi^2$, we have $2\sqrt{|\beta|}\xi = \int_0^u \frac{(u + \frac{2g}{\epsilon})du}{\sqrt{(r_1^2 - u)(r_2^2 - u)(r_3^2 - u)}}$. It gives rise to the following parametric representations of the periodic solutions:

$$\phi(\xi) = \pm \left(\frac{\alpha_2^2 r_1^2 \text{sn}^2(\omega_2 \xi, k)}{\alpha_2^2 \text{sn}^2(\omega_2 \xi, k) - 1} \right)^{\frac{1}{2}}, \tag{3.7}$$

where $\alpha_2^2 = \frac{-r_3^2}{r_1^2 - r_3^2}, k^2 = \frac{(r_2^2 - r_1^2)\alpha_2^2}{r_2^2}, \omega_2 = \frac{\epsilon\sqrt{|\beta|r_2^2(r_1^2 - r_3^2)}}{2g}$. For the periodic orbits that enclose equilibrium points $(\pm\phi_2, 0)$ and pass ϕ -axis at points $(\pm r_1, 0), (\pm r_2, 0)$, $\sqrt{|\beta|}\xi = \int_{r_2}^\phi \frac{(\phi^2 + \frac{2g}{\epsilon})d\phi}{\sqrt{(r_1^2 - \phi^2)(\phi^2 - r_2^2)(\phi^2 - r_3^2)}}$. Let $u = \phi^2$, we have

$$2\sqrt{|\beta|}\xi = \int_{r_2}^u \frac{(u + \frac{2g}{\epsilon})du}{\sqrt{(r_1^2 - u)(u - r_2^2)(u - r_3^2)u}},$$

and obtain the following parametric representations of the periodic solutions:

$$\begin{aligned} \phi(\chi) &= \pm \left(\frac{r_2^2 \operatorname{dn}^2(\chi, k)}{1 - \alpha_3^2 \operatorname{sn}^2(\chi, k)} \right)^{\frac{1}{2}}, \\ \xi(\chi) &= \frac{1}{r_2 \sqrt{|\beta|(r_1^2 - r_3^2)}} \left[(r_2^2 - r_3^2) \pi (\arcsin(\operatorname{sn}(\chi, k)), \alpha_3^2, k) + \left(\frac{2g}{\epsilon} + r_3^2 \right) \chi \right], \end{aligned} \tag{3.8}$$

where $\alpha_3^2 = \frac{r_1^2 - r_2^2}{r_1^2 - r_3^2}, k^2 = \frac{r_3^2 \alpha_3^2}{r_2^2}$.

The level curves defined by $H(\phi, y) = h_1$ contain two heteroclinic orbits which connect the saddle points $(\pm\phi_1, 0)$ and enclose the origin $(0, 0)$, two homoclinic orbits to the equilibrium points $(\pm\phi_1, 0)$ which pass ϕ -axis at $(\pm\phi_m, 0)$ and enclose two center points $(\pm\phi_2, 0)$ (see Fig.5 (d)). According to the two heteroclinic orbits, and

$$\begin{aligned} \sqrt{|\beta|} \xi &= \int_0^\phi \frac{(\phi^2 + \frac{2g}{\epsilon}) d\phi}{\sqrt{(\phi_m^2 - \phi^2)(\phi_1^2 - \phi^2)^2}} \\ &= \left[- \int_0^\phi \frac{d\phi}{\sqrt{\phi_m^2 - \phi^2}} + \left(\phi_1^2 + \frac{2g}{\epsilon} \right) \int_0^\phi \frac{d\phi}{(\phi_1^2 - \phi^2) \sqrt{\phi_m^2 - \phi^2}} \right]. \end{aligned}$$

We have the following parametric representations of the kink and anti-kink solutions:

$$\begin{aligned} \phi(\chi) &= \pm \left(\phi_1^2 - \frac{2\phi_1^2(\phi_m^2 - \phi_1^2)}{\phi_m^2 \cosh(\omega_3 \chi) - 2\phi_1^2 + \phi_m^2} \right)^{\frac{1}{2}}, \quad \chi \in (-\infty, +\infty) \\ \xi(\chi) &= \frac{-1}{\sqrt{|\beta|}} \left[\arcsin \frac{\phi}{\phi_m} + \frac{1}{2} \left(\phi_1^2 + \frac{2g}{\epsilon} \right) \chi \right], \end{aligned} \tag{3.9}$$

where $\omega_3 = \phi_1 \sqrt{\phi_m^2 - \phi_1^2}$. For the two homoclinic orbits,

$$\begin{aligned} \sqrt{|\beta|} \xi &= \int_\phi^{\phi_m} \frac{(\phi^2 + \frac{2g}{\epsilon}) d\phi}{\sqrt{(\phi_m^2 - \phi^2)(\phi^2 - \phi_1^2)^2}} \\ &= \left[\int_\phi^{\phi_m} \frac{d\phi}{\sqrt{\phi_m^2 - \phi^2}} + \left(\phi_1^2 + \frac{2g}{\epsilon} \right) \int_\phi^{\phi_m} \frac{d\phi}{(\phi^2 - \phi_1^2) \sqrt{\phi_m^2 - \phi^2}} \right]. \end{aligned}$$

Then, we obtain the parametric representations of homoclinic orbits solutions (see Fig.6 (b) and (c)):

$$\begin{aligned} \phi(\chi) &= \pm \left(\phi_1^2 + \frac{2\phi_1^2(\phi_m^2 - \phi_1^2)}{\phi_m^2 \cosh(\omega_3 \chi) + 2\phi_1^2 - \phi_m^2} \right)^{\frac{1}{2}}, \quad \chi \in (-\infty, +\infty) \\ \xi(\chi) &= \frac{1}{\sqrt{|\beta|}} \left[\frac{\pi}{2} - \arcsin \frac{\phi}{\phi_m} + \frac{1}{2} \left(\phi_1^2 + \frac{2g}{\epsilon} \right) \chi \right]. \end{aligned} \tag{3.10}$$

□

Theorem 3.2. *When $g\epsilon > 0$ and $c\gamma < 0$, we have phase portrait Fig.2. In this case, system (1.8) has little periodic wave solutions and solitary wave solutions. By*

using corresponding analyses, we have the following exact traveling wave solutions:

$$\begin{aligned} \phi(\chi) &= \pm \left(\frac{r_3^2}{1 - \alpha_4^2 \operatorname{sn}^2(\chi, k)} \right)^{\frac{1}{2}}, \\ \xi(\chi) &= \frac{1}{r_2 \sqrt{\beta(r_1^2 - r_3^2)}} \left[r_3^2 \pi(\arcsin(\operatorname{sn}(\chi, k)), \alpha_4^2, k) + \frac{2g}{\epsilon} \chi \right], \end{aligned} \tag{3.11}$$

where $r_3 < \phi_1 < r_2 < r_1$ are the intersection values of the level curves $H(\phi, y) = h$ and positive ϕ -axis, respectively, and $\alpha_4^2 = \frac{r_2^2 - r_3^2}{r_2^2}, k^2 = \frac{r_1^2 \alpha_4^2}{r_1^2 - r_3^2}$.

$$\begin{aligned} \phi(\chi) &= \pm \left(\phi_2^2 - \frac{2\phi_2^2(\phi_2^2 - \phi_m^2)}{\phi_m^2 \cosh(\omega_4 \chi) + 2\phi_2^2 - \phi_m^2} \right)^{\frac{1}{2}}, \quad \chi \in (-\infty, +\infty) \\ \xi(\chi) &= \frac{1}{\sqrt{\beta}} \left[\ln \phi_m - \ln |\phi + \sqrt{\phi^2 - \phi_m^2}| - \frac{1}{2}(\phi_2^2 + \frac{2g}{\epsilon})\chi \right], \end{aligned} \tag{3.12}$$

where ϕ_m is the intersection values of the right homoclinic orbit and ϕ -axis, $\omega_4 = \phi_2 \sqrt{\phi_2^2 - \phi_m^2}$.

Corresponding to Fig.3, system (1.8) exist three singular strait lines, as well as different saddles and nodes. Therefore, the system has very rich dynamic behaviors. That gives rise to various traveling wave solutions including periodic wave solutions, kink and anti-kink wave solutions and different periodic peakons. We obtain the following conclusion:

Theorem 3.3. *When $g\epsilon < 0$ and $c\gamma > 0$, corresponding to different bounded orbits in Fig.3 (a), (b), (c), (d), system (1.8) has different exact explicit solutions (3.13)-(3.19).*

Proof. (i) The case of $\hat{\alpha} < 0$.

System (1.8) has the phase portrait Fig.3 (a) and $\beta > 0$. The following Fig.7 (a)-(c) show the changes of the level curves:

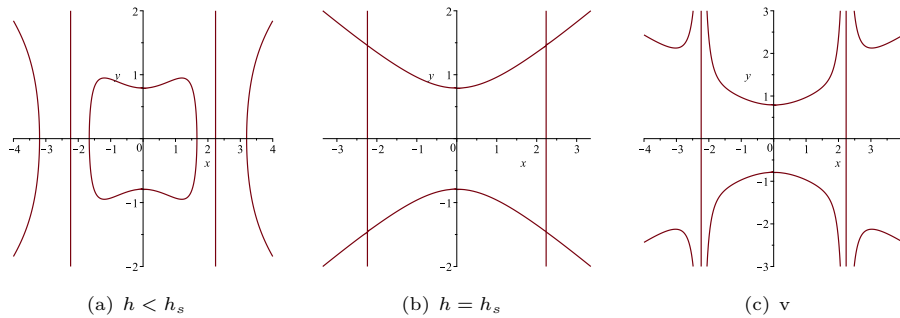


Figure 7. The changes of the level curves defined by (1.9) for $g\epsilon < 0, c\gamma > 0, \hat{\alpha} < 0$.

The level curves defined by $H(\phi, y) = h, h < h_s$ enclose two open curves passing the ϕ -axis at the $(\pm r_1, 0)$ and a family of periodic orbits enclosing the origin $(0, 0)$ (see Fig.7 (a)). For the periodic orbits, we have $\sqrt{\beta}\xi = \int_0^\phi \frac{-(\phi^2 + \frac{2g}{\epsilon})d\phi}{\sqrt{(r_1^2 - \phi^2)(\phi_2^2 - \phi^2)(\phi^2 + r_3^2)}}$.

Let $u = \phi^2$, we have $2\sqrt{\beta}\xi = \int_0^u \frac{-(u+\frac{2g}{\epsilon})du}{\sqrt{(r_1^2-u)(r_2^2-u)u(u+r_3^2)}}$. Then, the following parametric representations of the periodic solutions can be obtained:

$$\phi(\xi) = \pm \left(\frac{\hat{\alpha}_1^2 r_3^2 \text{sn}^2(\hat{\omega}_1 \xi, k)}{1 - \hat{\alpha}_1^2 \text{sn}^2(\hat{\omega}_1 \xi, k)} \right)^{\frac{1}{2}}, \tag{3.13}$$

where $\hat{\alpha}_1^2 = \frac{r_2^2}{r_2^2+r_3^2}$, $k^2 = \frac{\hat{\alpha}_1^2(r_1^2+r_3^2)}{r_1^2}$, $\hat{\omega}_1 = \frac{r_1 \epsilon \sqrt{\beta(r_2^2+r_3^2)}}{-2g}$.

Remark 3.1. The level curves defined by $H(\phi, y) = h_s$ are six arch segments (see Fig.7 (b)). When $h \rightarrow h_s$, the two segments between two straight lines $\phi = \pm\sqrt{\frac{-2g}{\epsilon}}$ are very closed to the two singular straight lines, so that the periodic solutions given by (3.13) give rise to a family of periodic peakons (see Fig.8).

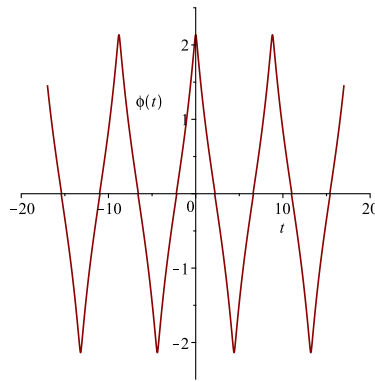


Figure 8. The periodic peakon or sawtooth cusp wave of system (1.8).

The level curves defined by $H(\phi, y) = h, h > h_s$ are six open curves (see Fig.7 (c)). For the two open curves between two singular straight lines $\phi = \pm\sqrt{\frac{-2g}{\epsilon}}$, we obtain from the first equation of system (1.8) that $\sqrt{\beta}\xi = \int_0^\phi \frac{-(\phi^2+\frac{2g}{\epsilon})d\phi}{\sqrt{(r_1^2+\phi^2)(\phi^2-\rho^2)(\phi^2-\bar{\rho}^2)}}$. Let $u = \phi^2$, we have $2\sqrt{\beta}\xi = \int_0^u \frac{-(u+\frac{2g}{\epsilon})du}{\sqrt{u(u+r_1^2)(u-\rho^2)(u-\bar{\rho}^2)}}$. The following parametric representations of the compact solutions can be obtained:

$$\begin{aligned} \phi(\chi) &= \pm \left(\frac{r_1^2 A (1 - \text{cn}(\chi, k))}{(A + B) \text{cn}(\chi, k) - A + B} \right)^{\frac{1}{2}}, \quad \chi \in (-\chi_1, \chi_1), \\ \xi(\chi) &= \frac{-1}{2\sqrt{\beta AB}} \left[\left(\frac{2g}{\epsilon} - \frac{r_1^2 A}{A + B} \right) \chi - \frac{r_1^2}{2\hat{\alpha}_2} \pi (\arccos(\text{cn}(\chi, k)), \frac{\hat{\alpha}_2^2}{\hat{\alpha}_2^2 - 1}, k) + \frac{r_1^2}{2} f_1 \right], \end{aligned} \tag{3.14}$$

where $a_1^2 = -\frac{1}{4}(\rho^2 - \bar{\rho}^2)^2$, $b_1 = \frac{1}{2}(\rho^2 + \bar{\rho}^2)$, $A^2 = b_1^2 + a_1^2$, $B^2 = (r_1^2 + b_1)^2 + a_1^2$, $k^2 = \frac{(A+B)^2 - r_1^4}{4AB}$, $\hat{\alpha}_2 = \frac{A+B}{B-A}$, $\chi_1 = \text{cn}^{-1} \left(\frac{r_1^2 A - \frac{2g}{\epsilon} (A+B)}{r_1^2 A - \frac{2g}{\epsilon} (A+B)} \right)$.

(ii) The case of $\hat{\alpha} > 0, \phi_1 < \frac{-2g}{\epsilon}$.

System (1.8) has the phase portrait Fig.3 (b) and $\beta < 0$. The level curves defined by $H(\phi, y) = h, h < h_1$ contain a family of periodic orbits enclosing the

origin point and four open curves passing the ϕ -axis at $(\pm r_1, 0), (\pm r_2, 0)$ where $r_1 > \sqrt{\frac{-2g}{\epsilon}} > r_2$. The family of global closed orbits have similar parametric representations as (3.7), where we use $-\omega$ instead of ω . For the open curves between two straight lines, they have the similar parametric representations as (3.8), where $\xi(\chi)$ needs an extra negative sign and $\chi \in (-\chi_2, \chi_2), \chi_2 = \text{sn}^{-1} \sqrt{\frac{2g+r_2^2}{\alpha_3^2(\frac{2g}{\epsilon}+r_3^2)}}$. Furthermore, according to the open curves which pass the ϕ -axis at $(\pm r_1, 0)$, we obtain $\sqrt{|\beta|}\xi = \int_{\phi}^{r_1} \frac{(\phi^2 + \frac{2g}{\epsilon})d\phi}{\sqrt{(r_1^2 - \phi^2)(\phi^2 - r_2^2)(\phi^2 - r_3^2)}}$. Let $u = \phi^2$, we have $2\sqrt{|\beta|}\xi = \int_u^{r_1^2} \frac{(u + \frac{2g}{\epsilon})du}{\sqrt{(r_1^2 - u)(u - r_2^2)(u - r_3^2)u}}$. It gives rise to the following parametric representations of the compact solutions(see Fig.9 (a) and (b)):

$$\begin{aligned} \phi(\chi) &= \pm \left(\frac{r_1^2}{1 - \hat{\alpha}_3^2 \text{sn}^2(\chi, k)} \right)^{\frac{1}{2}}, \quad \chi \in (-\chi_3, \chi_3), \\ \xi(\chi) &= \frac{1}{r_2 \sqrt{|\beta|(r_1^2 - r_3^2)}} \left[r_1^2 \pi(\arcsin(\text{sn}(\chi, k)), \hat{\alpha}_3^2, k) + \frac{2g}{\epsilon} \chi \right], \end{aligned} \tag{3.15}$$

where $\hat{\alpha}_3^2 = \frac{r_2^2 - r_1^2}{r_2^2}, k^2 = \frac{-\hat{\alpha}_3^2 r_3^2}{r_1^2 - r_3^2}, \chi_3 = \text{sn}^{-1} \sqrt{\frac{1 + \frac{\epsilon r_1^2}{2g}}{\hat{\alpha}_3^2}}$.

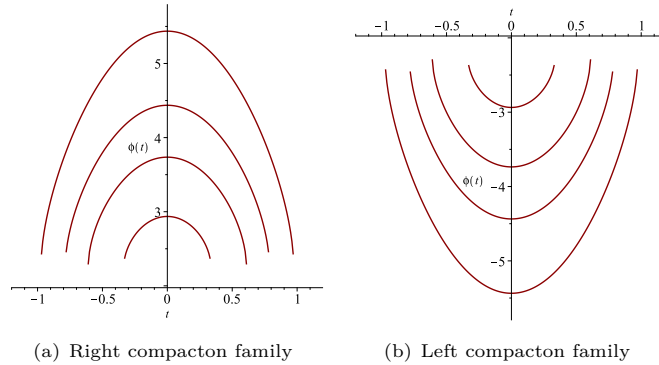


Figure 9. The compacton solution families of system (1.8).

The level curves defined by $H(\phi, y) = h_1$ are two heteroclinic orbits which connect the saddle points $(\pm\phi_1, 0)$ and enclose the origin $(0, 0)$, and two stable manifolds and two unstable manifolds to equilibrium points $(\pm\phi_1, 0)$, and two open curves passing the ϕ -axis at the $(\pm r_1, 0)$ where $r_1 > \sqrt{\frac{-2g}{\epsilon}}$. For the two heteroclinic orbits, we have the similar parametric representation as (3.9), where we use r_1^2 instead of ϕ_m^2 and $\xi(\chi)$ needs an extra negative sign. For the open curves which pass the points $(\pm r_1, 0)$, we have $\sqrt{|\beta|}\xi = \int_{\phi}^{r_1} \frac{(\phi^2 + \frac{2g}{\epsilon})d\phi}{\sqrt{(r_1^2 - \phi^2)(\phi^2 - \phi_1^2)^2}} = \left[\int_{\phi}^{r_1} \frac{d\phi}{\sqrt{r_1^2 - \phi^2}} + (\phi_1^2 + \frac{2g}{\epsilon}) \int_{\phi}^{r_1} \frac{d\phi}{(\phi^2 - \phi_1^2)\sqrt{r_1^2 - \phi^2}} \right]$. Therefore, we obtain the following

parametric representations of the compact solutions of system (1.8):

$$\begin{aligned} \phi(\chi) &= \pm \left(\phi_1^2 + \frac{2\phi_1^2(r_1^2 - \phi_1^2)}{r_1^2 \cosh(\hat{\omega}_2\chi) - r_1^2 + 2\phi_1^2} \right)^{\frac{1}{2}}, \quad \chi \in (-\chi_4, \chi_4), \\ \xi(\chi) &= \frac{1}{\sqrt{|\beta|}} \left[\frac{\pi}{2} - \arcsin \frac{\phi}{r_1} + \frac{1}{2}(\phi_1^2 + \frac{2g}{\epsilon})\chi \right], \end{aligned} \tag{3.16}$$

where $\hat{\omega}_2 = \phi_1 \sqrt{r_1^2 - \phi_1^2}$, $\chi_4 = \frac{1}{\hat{\omega}_2} \cosh^{-1} \left(\frac{r_1^2 \phi_1^2 - \frac{2g}{\epsilon}(r_1^2 - 2\phi_1^2)}{r_1^2(-\frac{2g}{\epsilon} - \phi_1^2)} \right)$.

The level curves defined by $H(\phi, y) = h, h > h_1$ enclose two open curves passing ϕ -axis at $(\pm r_1, 0)$ where $r_1 > \sqrt{\frac{-2g}{\epsilon}}$ and two open orbits passing y -axis at node points $(0, \pm \frac{|g|}{2\sqrt{c\gamma}})$, which tend to singular straight lines $\phi = \pm \sqrt{\frac{-2g}{\epsilon}}$ when $|y| \rightarrow \infty$, respectively. For the open curves passing y -axis, we obtain the similar parametric representations as (3.2) where $\xi(\chi)$ needs an extra negative sign and $\chi \in (-\chi_5, \chi_5), \chi_5 = \text{cn}^{-1} \left(\frac{B + \frac{2g}{\epsilon r_1^2}(A+B)}{B - \frac{2g}{\epsilon r_1^2}(A-B)} \right)$. According to the other two open curves, we have $\sqrt{|\beta|}\xi = \int_{\phi}^{r_1} \frac{(\phi^2 + \frac{2g}{\epsilon})d\phi}{\sqrt{(r_1^2 - \phi^2)(\phi^2 - \rho^2)(\phi^2 - \bar{\rho}^2)}}$, where ρ is a complex number. Let $u = \phi^2$, we have $2\sqrt{|\beta|}\xi = \int_u^{r_1^2} \frac{(u + \frac{2g}{\epsilon})du}{\sqrt{(r_1^2 - u)u(u - \rho^2)(u - \bar{\rho}^2)}}$. It gives rise to the following parametric representations of the wave solutions:

$$\begin{aligned} \phi(\chi) &= \pm \left(\frac{r_1^2 B(1 - \text{cn}(\chi, k))}{(A - B)\text{cn}(\chi, k) + A + B} \right)^{\frac{1}{2}}, \quad \chi \in (\chi_6, 2K(k)), \\ \xi(\chi) &= \frac{-1}{2\sqrt{|\beta|AB}} \left[\left(\frac{2g}{\epsilon} - \frac{r_1^2 B}{A - B} \right) \chi + \frac{A + B}{2B} \pi(\arccos(\text{cn}(\chi, k)), \frac{\hat{\alpha}_4^2}{\hat{\alpha}_4^2 - 1}, k) - \frac{r_1^2 B}{2A} f_1 \right], \end{aligned} \tag{3.17}$$

where $a_1^2 = -\frac{1}{4}(\rho^2 - \bar{\rho}^2)^2, b_1 = \frac{1}{2}(\rho^2 + \bar{\rho}^2), A^2 = (r_1^2 - b_1)^2 + a_1^2, B^2 = b_1^2 + a_1^2, k^2 = \frac{r_1^4 - (A - B)^2}{4AB}, \hat{\alpha}_4 = \frac{A - B}{A + B}, \chi_6 = \text{cn}^{-1} \left(\frac{B + \frac{2g}{\epsilon r_1^2}(A + B)}{B - \frac{2g}{\epsilon r_1^2}(A - B)} \right)$.

(iii) The case of $\hat{\alpha} > 0, \phi_1 = \frac{-2g}{\epsilon}$.

System (1.8) has the phase portrait Fig.3 (c) and $\beta < 0$. The level curves defined by $H(\phi, y) = h, h < h_1$ is a family of global closed orbits enclosing the origin $(0, 0)$ and passing the ϕ -axis at the $(\pm r_1, 0)$ where $r_1 < \sqrt{\frac{-2g}{\epsilon}}$. The periodic orbits have similar parametric representations as (3.4).

The level curves defined by $H(\phi, y) = h_1$ is one periodic orbit contacting two singular straight lines $\phi = \pm \sqrt{\frac{-2g}{\epsilon}}$ at equilibrium points $(\pm \sqrt{\frac{2g}{\epsilon}}, 0)$. For the periodic orbit, we have $y^2 = |\beta|(\frac{-2g}{\epsilon} - \phi^2)$. Thus, we have the following parametric representation of periodic wave solution:

$$\phi(\xi) = \pm \sqrt{\frac{-2g}{\epsilon}} \sin(|\beta|\xi). \tag{3.18}$$

(iv) The case of $\hat{\alpha} > 0, \phi_1 > \frac{-2g}{\epsilon}$.

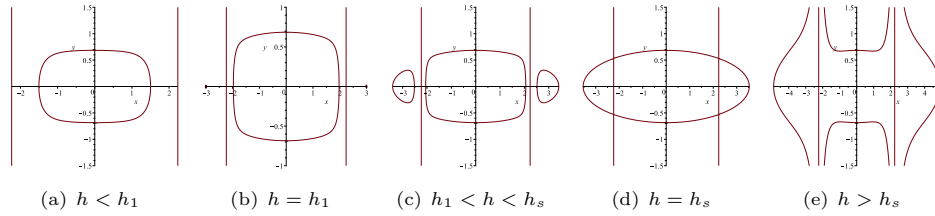


Figure 10. The changes of the level curves for $g\epsilon < 0, c\gamma > 0, \hat{\alpha} > 0, \phi_1 > \frac{-2g}{\epsilon}$.

System (1.8) has the phase portrait Fig.3 (d) and $\beta < 0$. The following Fig.10 (a)-(e) show the changes of the level curves:

The level curves $H(\phi, y) = h, h < h_1$ is a family of periodic orbits enclosing the origin point (see Fig.10 (a)). They have the same parametric representations as (3.4).

The level curves defined by $H(\phi, y) = h_1$ enclose two equilibrium points $(\pm\phi_2, 0)$ and one periodic orbit (see Fig.10 (b)). The periodic orbit have the same parametric representation as (3.6).

When $h_1 < h < h_s$, the level curves defined by $H(\phi, y) = h$ are there families of smaller periodic orbits (see Fig.10 (c)). They give rise to three families of smaller amplitude periodic wave solutions which have similar parametric representation as (3.5) and (3.6) respectively.

Remark 3.2. When $h \rightarrow h_s$, the family of periodic orbits enclosing the origin $(0, 0)$ give rise to the sawtooth periodic peakon, the two families of periodic orbits surrounding the centers $(\pm\phi_1, 0)$ give rise to the lower cusp wave solution and the upper cusp wave solution (see Fig.11 (a) and (b)).

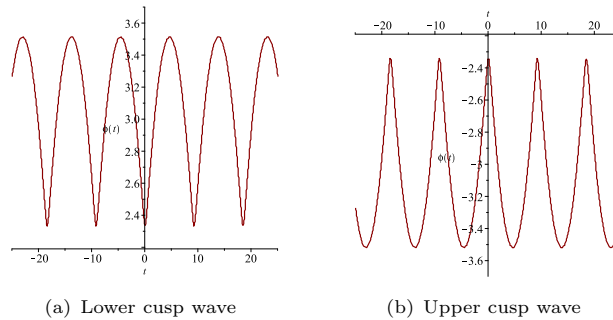


Figure 11. The periodic peakons of system (1.8).

The level curve defined by $H(\phi, y) = h_s$ is a larger periodic orbit, which enclose the origin $(0, 0)$ and two equilibrium points $(\pm\phi_1, 0)$, pass the ϕ -axis at the $(\pm r_1, 0)$ and two singular straight lines $\phi = \pm\sqrt{\frac{2g}{\epsilon}}$ at saddle points $(\pm\sqrt{\frac{2g}{\epsilon}}, \pm y_s)$, where $r_1 > \sqrt{\frac{-2g}{\epsilon}}$ (see Fig.10 (d)). We can obtain the following parametric representation

of large amplitude periodic wave solution:

$$\begin{aligned} \phi(\chi) &= \pm \left(\frac{r_1^2 B(1 - \text{cn}(\chi, k))}{(A - B)\text{cn}(\chi, k) + A + B} \right)^{\frac{1}{2}}, \quad \chi \in (-\chi_7, \chi_7), \\ \xi(\chi) &= \frac{-1}{2\sqrt{|\beta|AB}} \left[\left(\frac{2g}{\epsilon} - \frac{r_1^2 B}{A - B} \right) \chi + \frac{r_1^2}{2\hat{\alpha}_5} \pi(\arccos(\text{cn}(\chi, k)), \frac{\hat{\alpha}_5^2}{\hat{\alpha}_5^2 - 1}, k) - \frac{r_1^2}{2} f_1 \right], \end{aligned} \tag{3.19}$$

where $a_1^2 = -\frac{1}{4}(\rho^2 - \bar{\rho}^2)^2$, $b_1 = \frac{1}{2}(\rho^2 + \bar{\rho}^2)$, $A^2 = (r_1^2 - b_1)^2 + a_1^2$, $B^2 = b_1^2 + a_1^2$, $k^2 = \frac{r_1^4 - (A - B)^2}{4AB}$, $\hat{\alpha}_5 = \frac{A - B}{A + B}$, $\chi_7 = \text{cn}^{-1} \left(\frac{B + \frac{2g}{\epsilon r_1^2} (A + B)}{B - \frac{2g}{\epsilon r_1^2} (A - B)} \right)$. \square

Remark 3.3. In Fig.10 (d), two singular straight lines separate periodic orbit into four curve segments. The two curves segments between two singular straight lines $\phi = \pm\sqrt{\frac{2g}{\epsilon}}$ define the above sawtooth periodic peakon. The other two curve segments define the above lower cusp wave solution and upper cusp wave solution respectively (see Fig.11 (a) and (b)).

Theorem 3.4. *When $g\epsilon < 0$ and $c\gamma < 0$, we have phase portrait Fig.4. In this case, system (1.8) has little periodic wave solutions and compact wave solutions (3.20) and (3.21).*

Proof. (i) The case of $\hat{\alpha} > 0$, $\phi_1 < \frac{-2g}{\epsilon}$.

System (1.8) has the phase portrait Fig.4 (a) and $\beta > 0$. The level curves defined by $H(\phi, y) = h$, $h_1 < h < h_s$ are two families of periodic orbits passing ϕ -axis at the $(\pm r_2, 0)$, $(\pm r_3, 0)$ and enclosing the equilibrium points $(\pm\phi_1, 0)$, respectively, and two open curves passing ϕ -axis at points $(\pm r_1, 0)$, where $r_3 < r_2 < \sqrt{\frac{-2g}{\epsilon}} < r_1$. The periodic orbits have the similar parametric representation as (3.11) where $\xi(\chi)$ needs an extra negative sign.

The level curves defined by $H(\phi, y) = h_s$ are two open curves passing singular straight lines $\phi = \pm\sqrt{\frac{2g}{\epsilon}}$ at the saddle points $(\pm\sqrt{\frac{2g}{\epsilon}}, \pm y_s)$ respectively. Now, for the two open curves, we have $y^2 = \frac{(\phi^2 - r_1^2)(\phi^2 - \rho^2)(\phi^2 - \bar{\rho}^2)}{(\phi^2 + \frac{2g}{\epsilon})^2}$, where ρ is a complex number. Then, the segments of the curves between two singular straight lines have the following parametric representations:

$$\begin{aligned} \phi(\chi) &= \pm \left(\frac{r_1^2 B(1 + \text{cn}(\chi, k))}{(A + B)\text{cn}(\chi, k) - A + B} \right)^{\frac{1}{2}}, \quad \chi \in (-\chi_8, \chi_8), \\ \xi(\chi) &= \frac{-1}{2\sqrt{\beta AB}} \left[\left(\frac{2g}{\epsilon} - \frac{r_1^2 B}{A + B} \right) \chi - \frac{r_1^2 B(B - A)}{2A(A + B)} \pi(\arccos(\text{cn}(\chi, k)), \frac{\hat{\alpha}_5^2}{\hat{\alpha}_5^2 - 1}, k) \right. \\ &\quad \left. - \frac{r_1^2 B}{2A} f_1 \right], \end{aligned} \tag{3.20}$$

where $a_1^2 = -\frac{1}{4}(\rho^2 - \bar{\rho}^2)^2$, $b_1 = \frac{1}{2}(\rho^2 + \bar{\rho}^2)$, $A^2 = (r_1^2 - b_1)^2 + a_1^2$, $B^2 = b_1^2 + a_1^2$, $k^2 = \frac{(A + B)^2 - r_1^4}{4AB}$, $\hat{\alpha}_5 = \frac{A + B}{B - A}$, $\chi_8 = \text{cn}^{-1} \left(\frac{B - \frac{2g}{\epsilon r_1^2} (A - B)}{-B - \frac{2g}{\epsilon r_1^2} (A + B)} \right)$.

Remark 3.4. As a limit solution of a family of periodic orbits defined by $H(\phi, y) = h, h \in (h_1, h_s)$ when $h \rightarrow h_s$, the parametric representations (30) of two curve segments define the lower peakon solution and upper peakon solution of system (1.8), respectively.

When $h > h_s$, the level curves defined by $H(\phi, y) = h$ are four unbounded open curves, and two open curves between two singular straight lines $\phi = \pm\sqrt{\frac{-2g}{\epsilon}}$ passing ϕ -axis at points $(\pm r_1, 0)$ and tending the two singular straight lines when $y \rightarrow \infty$, which have the same parametric representations as (30).

(ii) The case of $\hat{\alpha} > 0, \phi_1 > \frac{-2g}{\epsilon}$.

System (1.8) has the phase portrait Fig.4 (c) and $\beta > 0$. The level curves defined by $H(\phi, y) = h_1$ contain two stable manifolds and two unstable manifolds to saddle points $(\pm\phi_1, 0)$, and two open curves between two singular straight lines $\phi = \pm\sqrt{\frac{2g}{\epsilon}}$ passing ϕ -axis at the $(\pm r_1, 0)$ and tending the two singular straight lines when $|y| \rightarrow \infty$. For the two open curves, we have $\sqrt{\beta}\xi = \int_{r_1}^{\phi} \frac{-(\phi^2 + \frac{2g}{\epsilon})d\phi}{\sqrt{(\phi^2 - r_1^2)(\phi_1^2 - \phi^2)^2}} = \left[\int_{r_1}^{\phi} \frac{d\phi}{\sqrt{\phi^2 - r_1^2}} + (\phi_1^2 - \frac{2g}{\epsilon}) \int_{r_1}^{\phi} \frac{d\phi}{(\phi_1^2 - \phi^2)\sqrt{\phi^2 - r_1^2}} \right]$. Therefore, we obtain the following parametric representations of the compactons:

$$\begin{aligned} \phi(\chi) &= \pm \left(\phi_1^2 - \frac{2\phi_1^2(\phi_1^2 - r_1^2)}{r_1^2 \cosh(\hat{\omega}_3 \chi) - r_1^2 + 2\phi_1^2} \right)^{\frac{1}{2}}, \\ \xi(\chi) &= \frac{1}{\sqrt{\beta}} \left[\ln |\phi + \sqrt{\phi^2 - r_1^2}| - \ln r_1 + \frac{1}{2}(\phi_1^2 + \frac{2g}{\epsilon})\chi \right], \end{aligned} \quad (3.21)$$

where $\hat{\omega}_3 = \phi_1 \sqrt{\phi_1^2 - r_1^2}$. □

4. Conclusion

In this paper, by using dynamical system method, we study all possible bifurcations of the singular traveling wave system (1.8), prove that Equ.(1.1) has at least 18 different exact traveling wave solutions, and obtain more richer dynamical behaviors for the system than references [5, 6, 12, 20, 21] which have used other methods. In particular, we give the singular traveling wave system of (1.1), and obtain a lot of new traveling wave solutions not given in [5, 6, 12, 13, 20, 21] which only study the regular system of (1.1) under some special parameter conditions. These new traveling wave solutions include sawtooth periodic peakons (3.5), (3.13), upper and lower periodic peakons (3.6), (3.18), compacton solutions (3.14), (3.16), (3.21), and some others. The results obtained in the paper are very helpful for the physical application of the coupled nonlinear wave Eqs.(1.1).

References

- [1] A. Biswas, M. Ekici, A. Sonmezoglu and R. T. Alqahtani, *Optical soliton perturbation with full nonlinearity for Fokas–Lenells equation*, *Optik*, 2018, 165, 29–34,
- [2] P. F. Byrd and M. D. Fridman, *Handbook of Elliptic Integrals for Engineers and Scientists*, Springer, Berlin, 1971.

- [3] J. Chehab and D. Dutykh, *On time relaxed schemes and formulations for dispersive wave equations*, AIMS Math., 2019, 4, 254–278.
- [4] C. Gu, *On the Backlund transformations for the generalized hierarchies of compound MKdV-SG equations*, Lett. Math. Phys., 1986, 12, 31–41.
- [5] C. Guha-Roy, *Solitary wave solutions of a system of coupled nonlinear equation*, J. Math. Phys., 1987, 28, 2087.
- [6] C. Guha-Roy, *Exact solutions to a coupled nonlinear equation*, Inter. J. Theor. Phys., 1988, 27, 447.
- [7] X. Hu and Z. Zhu, *A Backlund transformation and nonlinear superposition formula for the Belov-Chaltikian lattice*, J. Phys. A, 1998, 31, 4755–4761.
- [8] R. Hirota, X. Hu and X. Tang, *A vector potential KdV equation and vector Ito equation: soliton solutions, bilinear Backlund transformations and Lax pairs*, J. Math. Anal. Appl., 2003, 288, 326–348.
- [9] W. Li and X. Geng, *Darboux transformation of a differential-difference equation and its explicit solutions*, Chinese Phys. Lett., 2006, 23, 1361–1364.
- [10] S. Lou and J. Lu, *Special solutions from the variable separation approach: the Davey-Stewartson equation*, J. Phys. A, 1996, 29, 4209–4215.
- [11] Z. Liu and T. Qian, *Peakons of the Camassa-Holm equation*, Appl. Math. Model., 2002, 26, 473–480.
- [12] D. Lu and G. Yang, *Compacton solutions and peakon solutions for a coupled nonlinear wave equation*, Inter. J. Nonlinear Science, 2007, 4, 31–36.
- [13] X. Liu and C. He, *New exact solitary wave solutions of a coupled nonlinear wave equation*, Abstr. Appl. Anal., 2013, 1–7.
- [14] J. Li and G. Chen, *Bifurcations of travelling wave solutions for four classes of nonlinear wave equations*, Int. J. Bifurcation and Chaos, 2005, 15, 3973–3998.
- [15] J. Li and G. Chen, *On a class of singular nonlinear traveling wave equations*, Int. J. Bifurcation and Chaos, 2007, 17, 4049–4065.
- [16] J. Li, Y. Zhang and X. Zhao, *On a class of singular nonlinear traveling wave equations (II): an example of GCKdV equations*, Int. J. Bifurcation and Chaos, 2009, 19, 1955–2007.
- [17] J. Li, W. Zhou and G. Chen, *Understanding peakons, periodic peakons and compactons via a shallow water wave equation*, Int. J. Bifurcation and Chaos, 2016, 26(12), 1650207.
- [18] J. Li, *Singular Nonlinear Traveling Wave Equations: Bifurcations and Exact Solutions*, Science Press, Beijing, 2013.
- [19] W. Ma, *Complexiton solutions of the Korteweg-de Vries equation with selfconsistent sources*, Chaos Soliton Fract., 2005, 26, 1453–1458.
- [20] Y. Shang, *Explicit and exact solutions for a coupled nonlinear wave equation*, J. Ningxia University (Natural Science Edition), 2000, 21, 290–294.
- [21] X. Xu and J. Zhang, *New exact and explicit solitary wave solutions to a class of coupled nonlinear equation*, Commun. Nonlinear Sci., 1998, 3, 189–193.